https://dx.doi.org/10.1016/j.coelec.2023.101215

Recent advances in the *operando* structural and interface characterisation of electrocatalysts

Hao Zhang[1], Zhengyang Zhou[2], Qiong Lei[3], Tsz Woon Benedict Lo[1,3*]

Address

[1]State Key Laboratory of Chemical Biology and Drug Discovery, Department of Applied Biology and Chemical Technology, The Hong Kong Polytechnic University, Hong Kong, China

[2]State Key Laboratory of High Performance Ceramics and Superfine Microstructure, Shanghai Institute of Ceramics, Chinese Academy of Sciences, Shanghai 200050, China

[3]Department of Applied Physics, The Hong Kong Polytechnic University, Hong Kong, China

*Corresponding author: Tsz Woon Benedict Lo (benedict.tw.lo@polyu.edu.hk)

Keyword

Operando characterisation, Powder X-ray diffraction, Raman spectroscopy, Electrocatalysis

Abstract

Using multiple *operando* characterisation techniques to elucidate the structure-reactivity correlations of electrocatalytic systems is becoming more desirable. In this review article, we primarily employed the electrocatalytic CO_2 reduction reaction over nanocatalysts as a model reaction to discuss the recent advances in the use of *operando* characterisation techniques. The synergy between various techniques can circumvent, to a great extent, the limitations of using one sole technique. For instance, the advances in using a combination of *operando* powder X-ray diffraction and Raman spectroscopy are discussed, which enables the complementary characterisation of nanocatalysts in both bulk and surface levels. Under *operando* conditions, the adsorbate and intermediate species, as well as the structural parameters of the catalyst can be simultaneously tracked for an extensive understanding of the reaction mechanisms.

Introduction

Deciphering the relationship between the structure of catalytic materials and catalytic reactivity is pivotal to designing new-generation catalytic materials with superior performance [1–5]. Rational design-driven catalysts with high selectivity towards target products could fundamentally alleviate the current harsh energy demand and environmental issues [6–9]. In recent years, with the rapid development of instrumentations, numerous advanced characterisation techniques have continuously refreshed our understanding of catalytic reactions. These state-of-the-art characterisation techniques, especially those that allow *operando* characterisation, have offered us special perspectives (i) to reveal the dynamic structural change of the catalysts [10–12], (ii) to unveil the catalytic mechanism occurring at the interface of the

solid catalyst *via* tracking of preferential adsorbate species or reaction intermediates [13,14], or (iii) both combined [15,16]. At this point, we should first clarify the difference between two commonly misused adjectives – *operando* and *in-situ*. First, '*operando*' can be considered as a subset of '*in-situ*'. The former refers to 'under operating conditions'; in the context of the electrocatalytic CO_2 reaction reduction ('eCO_2RR', which is used as one of the model reactions in this short review), *operando* characterisation generally should be conducted under (i) applied voltage, (ii) flowing CO_2, and (iii) immersed in electrolytes. In some cases, reasonable deviations from the 'real' operating conditions of electrocatalysis are unavoidable, *e.g.*, dilution of the electrolyte, because of various intrinsic limitations of the system. Product analysis is desired to ensure the behaviour of the *operando* catalytic system. In contrast, *in-situ* characterisation is the study of the catalyst at various applied stimuli. A typical example can be studying the structural evolution during the calcination process. Understanding the intermediate alternation and the structural evolution of catalysts can offer a step closer towards an actual realisation of the 'chemical/molecular movies' [17–19]. Every 'frame' could be employed to form a complete data chain, which provides valuable information for guiding scientists towards further materials engineering and system optimisation.

Despite the capability of individual *in-situ* and *operando* characterisation techniques has been well discussed in some recent articles *[5], this review will focus on discussing the combination of using powder X-ray diffraction (PXRD) and Raman spectroscopy in studying electrocatalytic reactions, considering the eCO_2RR over various Cu-based catalysts for example, under *operando* conditions. As shown in Figure 1, whereas PXRD can detect the change in the bulk structure, such as phase change, Raman spectroscopy, by applying a suitable laser, can reveal the surface and interface chemistry. These two core characterisation techniques can be applied together to offer complementary information about the catalysts, thereby elucidating the structure-reactivity correlations with a more multifaceted perspective.

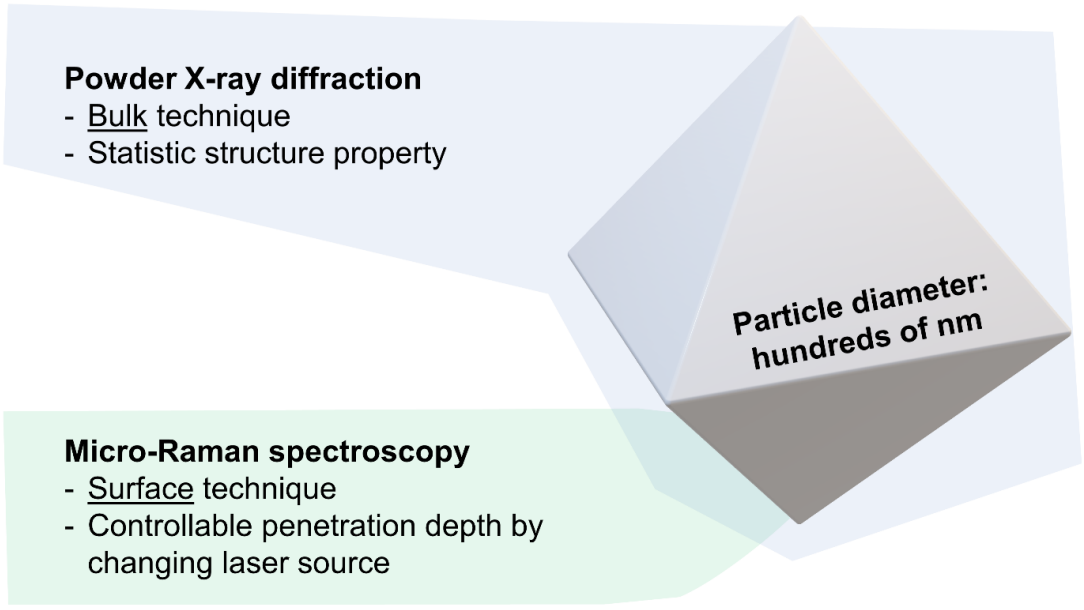

Figure 1. Major *operando* characterisation techniques discussed in this article, where both the bulk and surface properties of electrocatalysts, such as in the form of nanoparticles, can be simultaneously studied.

Operando PXRD

PXRD is a conventional technique that is often present in most laboratories and extensively used by most researchers working on solid materials [20–22]. By observing Bragg's law, PXRD is typically used for fingerprint identification of materials, and characterisation of the structural parameters, such as lattice type, unit cell parameter, and lattice strain [23]. *Ex-situ* PXRD measurements of solid samples are generally measured in reflection or transmission mode, where the samples are well-aligned between the X-ray beam and detector to yield accurate and precise information. However, when it is applied to *operando* (or most *in-situ*) settings, a series of limitations should first be noted [24]. The major limitation is the intense absorption issue of X-ray when the X-ray beam passes through the electrolyte. Even using synchrotron X-ray, with much higher X-ray brilliance (photons s^{-1} mm^{-2} $mrad^{-2}$/0.1%BW), the electrolyte issue is also a major hurdle for the design of a suitable reactor cell. As noted in our recent study on the hydrogen evolution reaction over $NiSe_2$ (which will be later discussed), 1.0 M KOH electrolyte with a thickness of 5 mm was required to be diluted substantially (to 0.1 M) for reasonable transmission mode measurements [25]. Even still, the background signal of the diluted electrolyte can be extremely high which could interfere with the detection of Bragg's peaks. Both water and salt present in the electrolyte are strong X-ray absorbers. When designing a reactor cell that uses a conventional laboratory X-ray source (3 kW, or even 9 kW), the presence of trace electrolytes will be detrimental which can severely hamper the detection of the scattered X-ray. Based on our experience, the Bragg's peaks are barely observable simply with a drop of water on top of the electrode (catalyst). We should ensure minimal contact between the X-ray beam and electrolyte to achieve a high signal-to-noise ratio.

As shown in Figure 2, we show an illustration of an example eCO_2RR reactor cell where the stringent requirements of both CO_2 conditions (gas flow, electrode contact, *etc.*), electrochemical (comparable current densities), and diffraction environments (sample and optical alignments, *etc.*) can be simultaneously met **[26]. Another major limitation is that PXRD is only suitable for the detection (and quantification) of the crystalline phase(s), it is extremely challenging to exclude the possible presence of metastable, short-lived, amorphous oxidised species in the sample under such dynamic measurement.

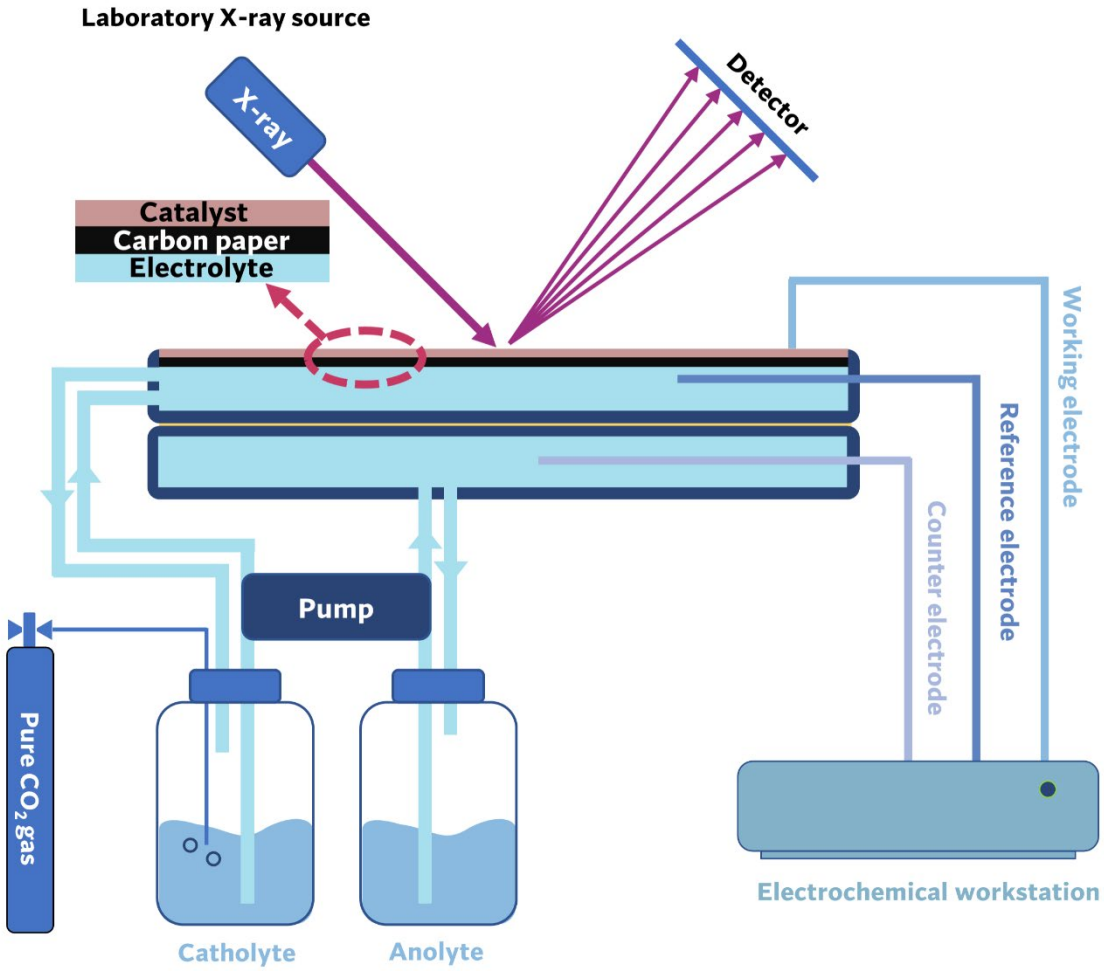

Figure 2. Schematic illustration of an *operando* PXRD reactor cell (reflection mode).

In recent years, *operando* PXRD has been employed to study dynamic changes, such as phase transition [27–29] and lattice strain [30–32] under electrochemical environments. In another matter, *operando* studies using grazing incidence X-ray diffraction-based technique can also be done to yield information on the dynamic structural change on the surface and sub-surface species of the catalyst by limiting the penetration of X-ray to the bulk structure [33]. In this section, we have selected two examples to illustrate the application of *operando* PXRD in the study of the dynamic change of the electrolyte.

Ni-based chalcogenides have been regarded as a promising class of electrocatalysts for efficient hydrogen evolution reaction (HER) in an alkaline environment. It is often understood that metallic Ni, as reduced from NiS_2 or $NiSe_2$, is the actual 'active species' for HER [34]. Unaltered Ni-based chalcogenides, morphologically and compositionally, should not long remain upon applied potentials. In the work by Zhai *et al.*, *operando* synchrotron PXRD was employed to characterise the phase transition of the $NiSe_2$ catalyst for HER (Figure 3) **[35]. Initially, the identity of the pristine sample $NiSe_2$ was first confirmed by the characteristic Bragg peaks at 10.7° (210), 13.6° (220), and 15.9° (311). Under the applied voltage at –0.18 V in diluted 0.1 M KOH electrolyte~~)~~, a gradual decrease of these Bragg peaks (of $NiSe_2$) was noted. The Bragg peaks characteristic of NiSe gradually appeared and became more dominant after two hours of time-on-

stream, while the Bragg peaks of $NiSe_2$ disappeared completely, which was accompanied by an increase in the current density by 27.3%. No further phase evolution was observed beyond two hours based on a 24-hour chronoamperometric measurement. This hence confirmed that NiSe acted as the 'active species' in their catalyst system. It suggests the introduction of compressive forces on the *b*-*c* surface and drawing forces on the *a*-*b* surface, which could be related to the electric stress and interaction with neighbouring $NiSe_2$ domains or nanocrystallites.

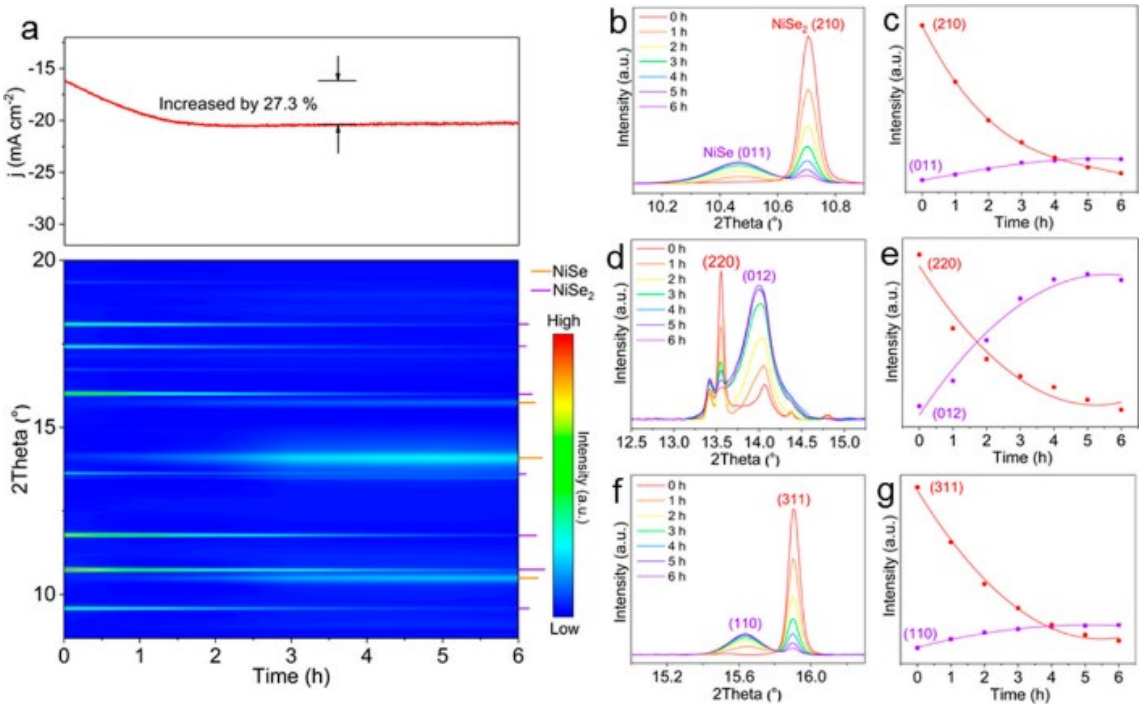

Figure 3. (a) Current curve at −0.18 V for 6 h and the corresponding *operando* synchrotron PXRD patterns of the $NiSe_2$. (b–g) Enlarged fingerprint peaks and corresponding intensity evolution. (Reprinted with permission from ref.[35]. Copyright © 2020, American Chemical Society)

Similar phase evolution observations, but at faster reduction rates, were also noted under higher biased potentials at –0.38 V and –0.58 V. Potentially due to electron transportation and environmental issues, the authors found that the peaks of NiSe at –0.58 V were much broader, indicative of smaller lattice domains. The author further correlated the structure-reactivity pattern between catalysis and phase evolution. By density functional theory calculations, the $NiSe_2$ to Ni transition upshifts the *d*-band centre to closer to that of Pt (–1.93 eV), which made it much more suitable for HER.

Nevertheless, sample oxidation should not be excluded, as hydroxide formation (such as due to ambient exposure) has also been commonly reported by various *ex-situ* post-catalytic measurements [36]. The identification of the NiSe phase was successful as the *operando* characterisation effectively circumvented the subtle reactions if the sample were measured *ex-situ* post reactions. However, it should also be noted the limitation of using reactor cells – a transmission cell in this case, where the sample was fully immersed in KOH electrolyte. The concentration of the KOH electrolyte was specifically diluted to 0.1 M from 1.0 M to reduce the X-ray absorption issue for enhanced counting statistics.

Lei *et al.* investigated the origin of the difference in the eCO_2RR catalytic selectivity over nano Cu catalysts when different Cu precursors, CuO, $Cu(OH)_2$ and $Cu_2(OH)_2CO_3$, were used [26]. Unlike the previous transmission mode reactor cell used by Zhai *et al*., an eCO_2RR reactor cell optimised for PXRD measurements in the reflection mode was designed. The reflection mode was specifically needed because of laboratory-grade X-ray source was used, with a much lower X-ray brilliance compared with synchrotron X-ray. It has also been particularly noted that the catalytic behaviour of the reactor cell was corrected using a standard sample to eliminate liquid-induced effects.

The Bragg peaks characteristic of the Cu precursors gradually vanished upon an applied potential, while those characteristics of metallic Cu species (*e.g.*, Cu(111) at 2θ = ~ 43.3° and Cu(200) at 2θ = ~ 50.3°) emerged after 15 minutes of time-on-stream. All three Cu precursors were subsequently reduced to metallic Cu, but with different electrochemical reduction kinetics. Comparable domain/grain sizes of ~ 11 nm were observed. The observed domains were notably smaller than the parent Cu precursor materials, which was attributed to the combined effect of the lattice shrinkage and fragmentation of the nanocrystallites. It was concluded that the formation of these as-reduced metallic Cu species, with less relevance to the identity of the Cu precursors, was pivotal to explaining the enhanced and comparable C_{2+} selectivity in the eCO_2RR.

Lei *et al.* also discovered the presence of tensile strain (measured by peak shift of the Bragg peaks) only in the metallic Cu species derived from $Cu(OH)_2$ and $Cu_2(OH)_2CO_3$ precursors by > 0.4% [26]. Such tensile strains could only be probed using the *operando* technique, as the shifts of the Bragg peaks were not observed in their *ex-situ* PXRD measurements.

Operando Raman Spectroscopy

Compared with PXRD (bulk technique), Raman spectroscopy is more inclined to the study of the surface adsorbate and intermediate species, as well as tracking the structural parameters of the catalyst surface [37–40]. When a single-wavelength laser is irradiated on the surface of the nanocrystallites, inelastically scattered light is generated depending on the spin and vibration of the species with molecular behaviours. In addition to the well-known (*ex-situ*) capabilities of Raman spectroscopy, the laser can penetrate through a thin layer of typical electrolytes with low Raman scattering cross sections [41]. Low Raman scattering cross sections enable the characterisation of the electrode/electrolytes interface, where electrolysis takes place, with higher accuracy and reliability. Also, this warrants more ‘realistic’ *operando* conditions to be met for the design of Raman reactor cells. However, Raman spectroscopy is not intrinsically surface (more specifically interface) active. The surface-enhanced Raman spectroscopy (SERS) has been accordingly designed to allow the identification of the interface adsorbate and intermediate species, as it can enhance the interface-related signals by 10^{10}-10^{11} times [42,43]. But still, there are some intrinsic limitations when *in-situ*/*operando* conditions are applied, such as most dynamic information is lost after removing the catalyst from electrocatalysis conditions due to thermodynamic relaxation of the materials during preparation for analysis, and the difficulty in conducting measurements with high reproducibility under various

environments **[44]. Figure 4 illustrates the design of a typical commercial *operando* Raman reactor cell.

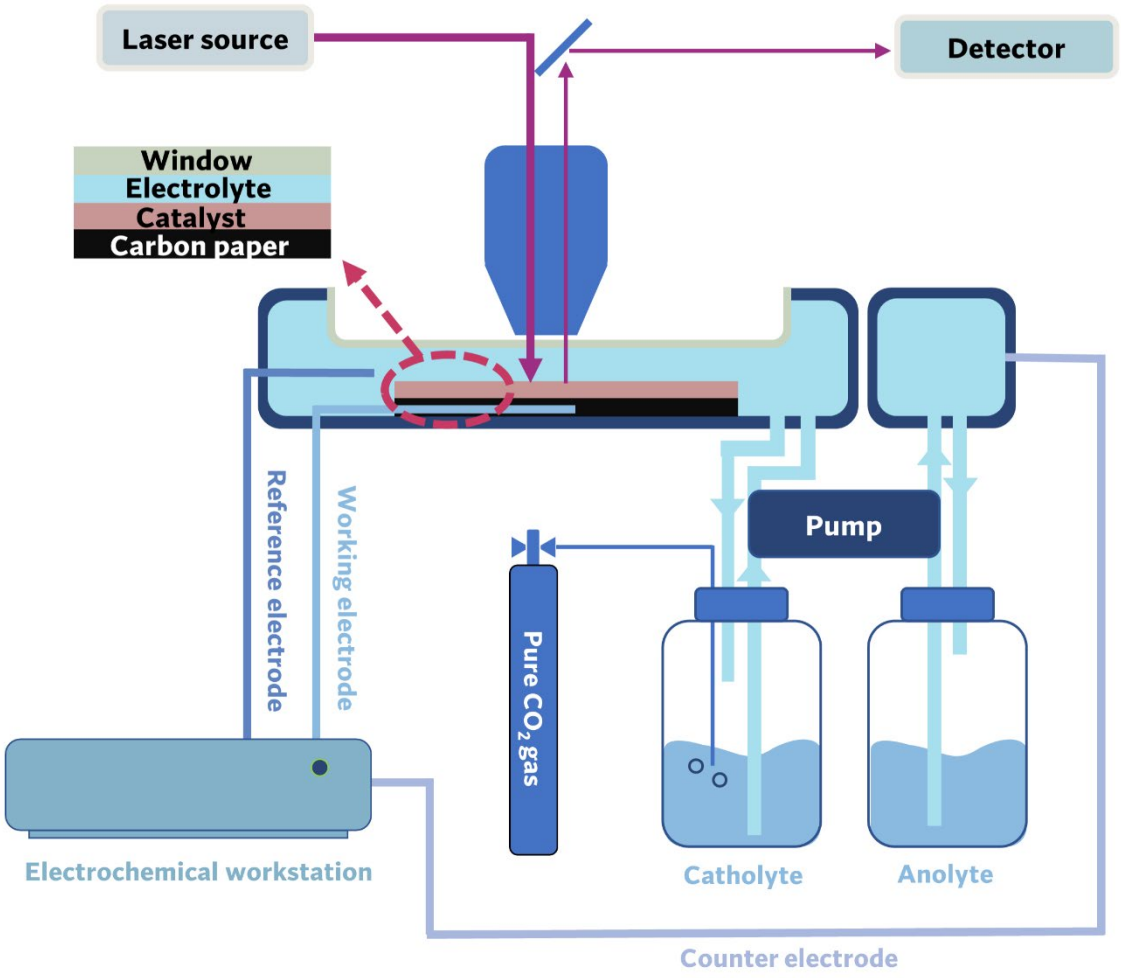

Figure 4. Schematic illustration of an *operando* SERS reactor cell. A thin layer of water can be allowed above the catalyst surface because of laser can penetrate through the electrolyte at a reasonable electrolyte concentration.

The benefits of oxides on metal copper surfaces have been recognised by the community as they can enhance the catalytic efficiency of multicarbon C_{2+} products [45–47]. However, the lack of powerful characterisation tools and the inability to control these oxygen-containing species hinder understanding the role of these oxide species in the eCO_2RR.

Inspired by this, He *et al*. employed *operando* SERS spectroscopy to probe the Cu surface speciation in H_2O_2-contained electrolytes as a function of voltages **[48]. As shown in Figure 5, in 0.1 M $KHCO_3$ + 5 mM H_2O_2, the fingerprint peaks of Cu_2O at 146, 412, 528, and 619 cm^{-1} remained until –0.3 V_{RHE}, compared to without H_2O_2, Cu_2O is more prone to reduction reduced even at 0 V_{RHE}. It suggested that the stabilisation of the surface oxide species by H_2O_2. They also found that the peak at 1070 cm^{-1} appeared after the reduction of Cu_2O and remained visible at a more negative voltage

with the addition of H_2O_2, which is likely attributed to the favourable adsorption of CO_3^{2-} on the as-reduced metallic copper.

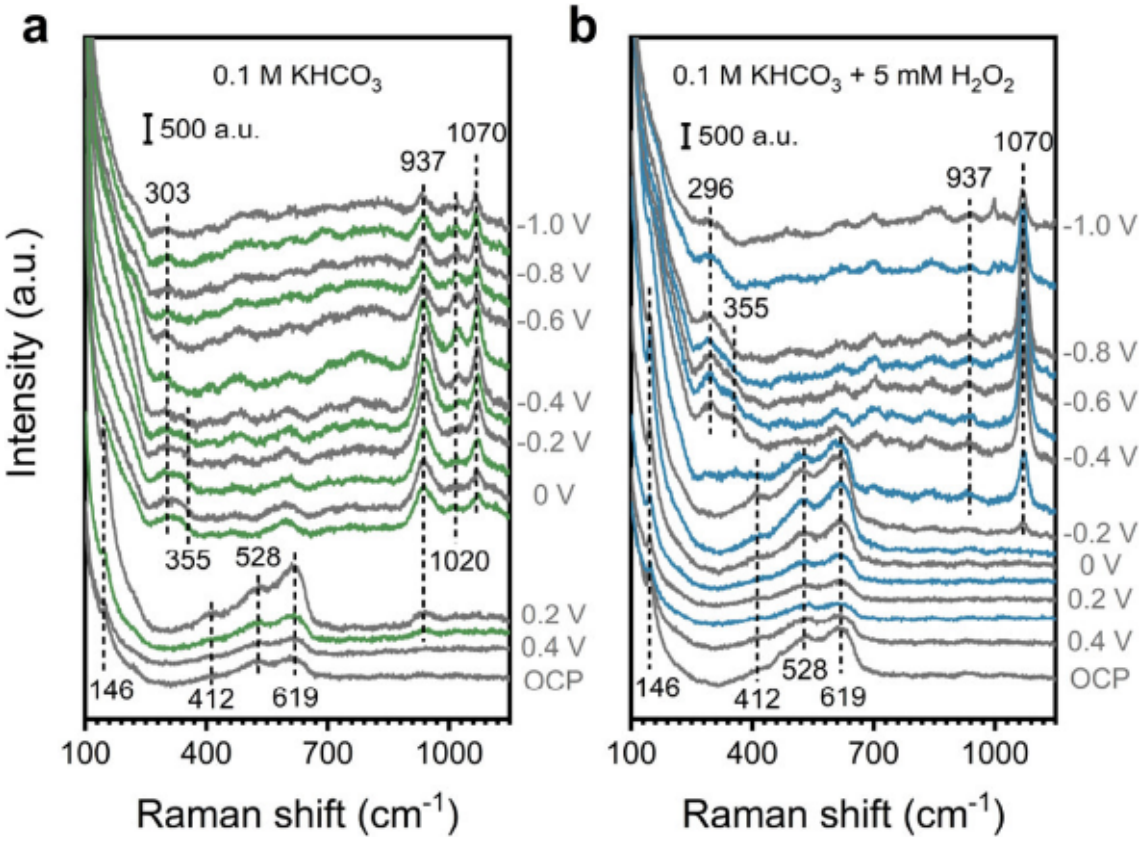

Figure 5. Potential-dependent *operando* SERS. Shell-isolated nanoparticle-enhanced Raman spectra of electropolished Cu foil acquired at different potentials in (a) 0.1 M $KHCO_3$ and (b) 5 mM H_2O_2 + 0.1 M $KHCO_3$. The electrolyte was continuously purged with CO_2 during electrolysis. (Reprinted with permission from ref.[48]. Copyright 2022, American Chemical Society)

Furthermore, the time-dependent *operando* SERS results (Figure 6) suggested that the presence of H_2O_2 could guide the formation of oxygen-containing species on the copper surface under the eCO_2RR condition. The peak at 525 cm^{-1}, which was assigned to $CuO_x(OH)_y$, appeared after 10 min and increased in intensity until the addition of 20 µL H_2O_2 after 50 minutes. This peak disappearance was resulted from the $CuO_x(OH)_y$ species being oxidised to Raman inactive Cu oxide species by H_2O_2, which could further stabilised on the copper surface for an extended time. From the results of the DFT calculations, the authors found that the *CO hydrogenation was more thermodynamically and kinetically favourable on the Raman inactive Cu oxide species compared to bare metallic copper.

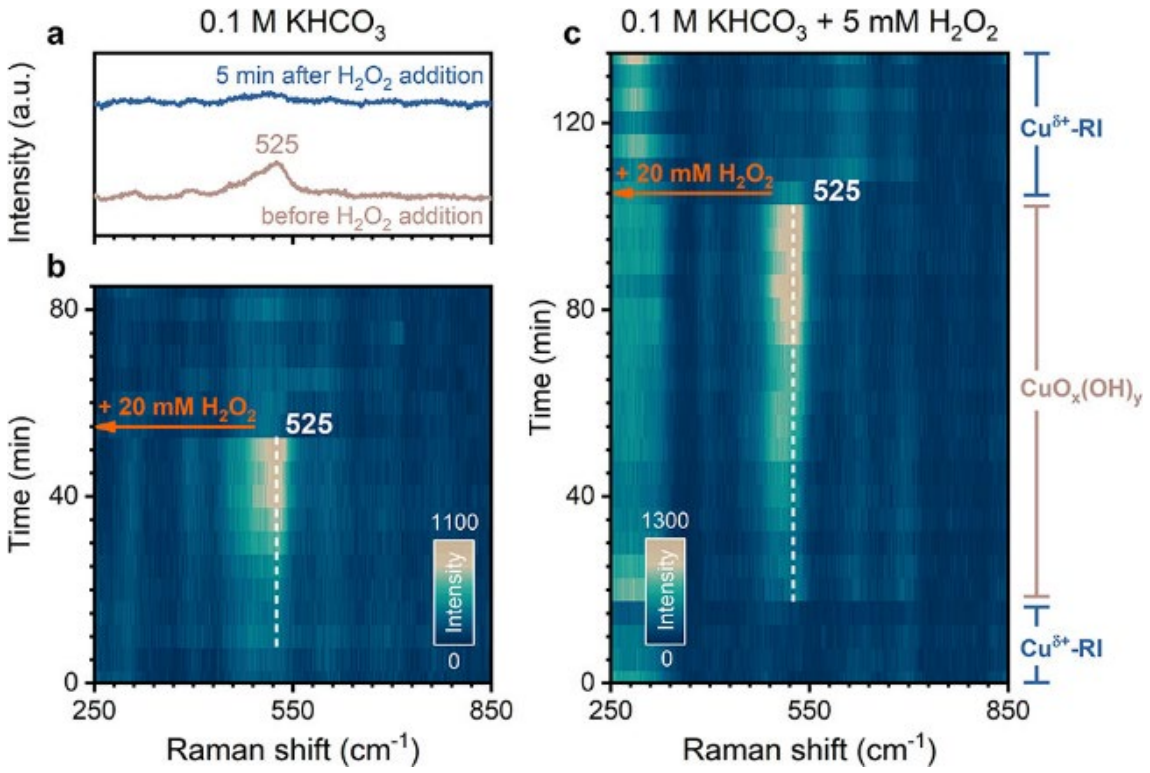

Figure 6. Time-resolved *in-situ* SERS at −1.0 V_{RHE}. (a) Representative SER spectra acquired before and after H_2O_2 addition (at 50- and 60-min electrolysis, respectively) in 0.1 M $KHCO_3$, (b) time-resolved SER spectra acquired in 0.1 M $KHCO_3$ with 20 mM H_2O_2 added to the electrolyte at 55 min, (c) time-resolved SER spectra acquired in 5 mM H_2O_2 + 0.1 M $KHCO_3$ with an additional of 20 mM H_2O_2 added to the electrolyte at 105 min. The electrolyte was constantly purged with CO_2 during electrolysis. (Reprinted with permission from ref.[48]. Copyright 2022, American Chemical Society)

An *et al*. employed *operando* SERS to study the reaction mechanism of eCO_2RR on the Cu metal surface and by tracking *CO intermediates **[49]. Taking advantage of the sub-second detection capability of this approach, the vibration peaks at 524 and 614 cm^{-1} disappeared immediately (within the first few seconds), even at a low voltage of –0.4 V (Figure 7). This suggested that the copper oxide species was stripped from the Cu metal, and the reaction site activation was also completed at once.

These catalysts showed higher selectivity at more negative operation voltage at –0.8 V_{RHE} and −0.9 V_{RHE}. As shown in Figure 7a, the characteristic peak of low-frequency band liner CO at 2060 cm^{-1} gradually increased, while the relative intensity of high-frequency band liner CO at 2095 cm^{-1} decreased, with the peak shifted to a lower wavelength. The time-dependent changes in the peak positions indicated that the CO* intermediates on the catalyst surface were highly dynamic and actively participated in surface reactions rather than static steady-state adsorption (Figure 7b-d). The lower Raman wavelength suggested a weaker C=O bond, which could promote the dimerisation of CO* intermediates and play an essential role in the subsequent formation of multi-carbon C_{2+} products (Figure 7e). It is almost impossible to record this dynamic state and peak shift with conventional Raman spectroscopy as the lifetime of *CO intermediates is relatively short under *ex-situ* conditions.

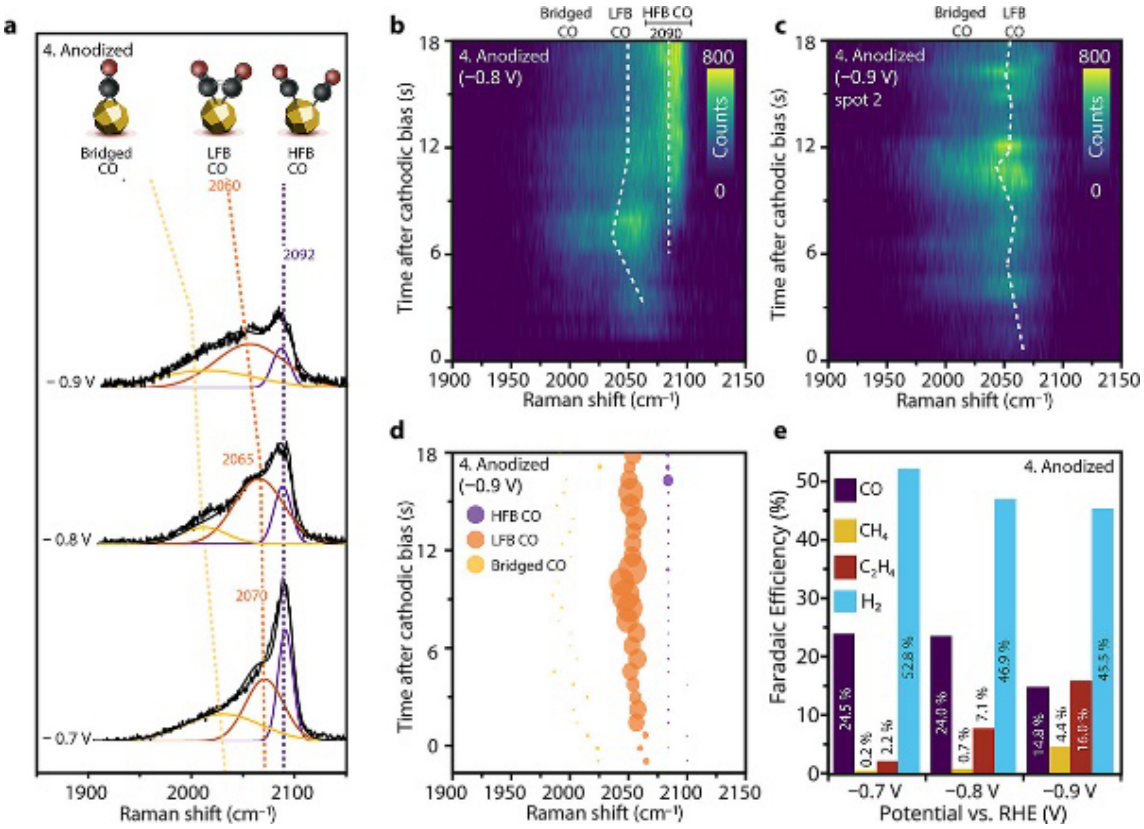

Figure 7. (a) Comparison of steady-state Raman spectra (15 min after reduction) of anodised Cu-MP during reduction at −0.7 V, −0.8 V and −0.9 V. Collection time is 5 s. Time-resolved surface-enhanced Raman spectroscopy heatmap of (b) anodised Cu-MP during reduction at −0.8 V and (c) −0.9 V in the CO region (Raman shift between 1900-2150 cm^{-1}). (d) Fitted result of (c), (e) FE of anodised Cu-MP during eCO_2RR at −0.7 V, −0.8 V, and −0.9 V. (Reprinted from ref. [49], with permission from Wiley, copyright 2021)

Summary

In this review, we discussed the advantages of using *operando* PXRD and Raman spectroscopy for the characterisation of electrocatalytic reactions (primarily using eCO_2RR as a model reaction). They can extensively complement each other and can characterise nanocrystalline catalysts from both bulk and surface levels. Under the conditions of real-time monitoring, the adsorbate and intermediate species, as well as the structural parameters of the catalyst can be simultaneously tracked. It offers a combined perspective for a thorough understanding of the catalytic system, and subsequently, aids the rational design of more efficient catalysts.

Although combining these two techniques can help us study the principles of electrocatalytic reactions from a deeper perspective, it is still impossible to fully understand the effects of all parameters on the catalytic reactions. Most current laboratory *operando* PXRD reactor cells adopt the indirect connection method, which extracts water onto the carbon paper (electrode) to form a closed-loop circuit to avoid water suppression of X-ray. It is challenging to make catalysts fully immersed in the electrolyte, even with the use of synchrotron X-ray with a much higher beam brilliance. The time resolution is also limited by the duration of each PXRD scan, which causes more issues in *operando* PXRD measurements as a quick non-synchrotron scan require at least a few minutes for acceptable-quality data collection.

Laser-induced sample damage is common from overexposure in Raman spectroscopy (which could be alleviated by developing a more sensitive detector to lower the laser power). It thus limits ultra-long measurements where a high volume of data acquisitions is involved. In addition, many intermediate species on the catalyst surface cannot be characterised by *operando* Raman spectroscopy. A possible solution is to adopt complementary *operando* infrared spectroscopy to track those intermediate species of interest. Another limitation is the lack of quantification ability by Raman spectroscopy as the peak intensity does not fully reflect the population of the species of interest. In brief, when designing *operando* reactor cells, particularly for junior and less-experienced researchers, one should expect at least a couple of months for proper cell optimisation. But once a cell is optimised and commissioned, it would offer you an extremely powerful tool to understand your catalytic system(s).

Funding sources
TWBL thanks the Department of Science and Technology of Guangdong Province (2021A1515010218), the National Natural Science Foundation of China (22172136), the Hong Kong Research Grants Council (15301521 and 15300819), and PolyU start-up SHS fund (BDC3), for financial support.

Reference

[1] L. Ye, P. Zhao, M.M.J. Li, B.T.W. Lo, C. Tang, S.C.E. Tsang, Evaluation of the molecular poisoning phenomenon of W sites in ZSM-5 via synchrotron X-ray powder diffraction, Chem. Commun. 54 (2018) 7014–7017.

[2] B.T.W. Lo, L. Ye, J. Qu, J. Sun, J. Zheng, D. Kong, C.A. Murray, C.C. Tang, S.C.E. Tsang, Elucidation of Adsorbate Structures and Interactions on Brønsted Acid Sites in H-ZSM-5 by Synchrotron X-ray Powder Diffraction, Angew. Chem. Int. Ed. 55 (2016) 5981–5984.

[3] B.T.W. Lo, L. Ye, S.C.E. Tsang, The Contribution of Synchrotron X-Ray Powder Diffraction to Modern Zeolite Applications: A Mini-review and Prospects, Chem 4 (2018) 1778–1808.

[4] B.T.W. Lo, L. Ye, C.A. Murray, C.C. Tang, D. Mei, S.C.E. Tsang, Monitoring the methanol conversion process in H-ZSM-5 using synchrotron X-ray powder diffraction-mass spectrometry, J. Catal. 365 (2018) 145–152.

*[5] X. Li, S. Wang, L. Li, Y. Sun, Y. Xie, Progress and Perspective for in Situ Studies of CO_2 Reduction, J. Am. Chem. Soc. 142 (2020) 9567–9581.

The authors highlights some recent progress for in-situ studies of CO_2 reduction. Based on the achievements in some representative studies, the authors presented some prospects and suggestions for in-situ studies of CO_2 reduction in the future.

[6] Q. Xue, B.K.Y. Ng, H.W. Man, T.S. Wu, Y.L. Soo, M.M. Li, S. Kawaguchi, K.Y. Wong, S.C.E. Tsang, B. Huang, T.W.B. Lo, Controlled synthesis of Bi- and tri-nuclear Cu-oxo nanoclusters on metal–organic frameworks and the structure–reactivity correlations, Chem. Sci. 13 (2021) 50–58.

[7] T. Chen, Q. Xue, K.C. Leung, B.T.W. Lo, Recent Advances of Precise Cu Nanoclusters in Microporous Materials, Chem. Asian. J. 15 (2020) 1819–1828.

[8] T. Chen, C.K.T. Wun, S.J. Day, C.C. Tang, T.W.B. Lo, Enantiospecificity in achiral zeolites for asymmetric catalysis, Phys. Chem. Chem. Phys. 22 (2020) 18757–18764.

[9] B.T.W. Lo, W. che Lin, M.M.J. Li, S. Day, C. Tang, S.C.E. Tsang, Evaluation of Brønsted and Lewis acid sites in H-ZSM-5 and H-USY with or without metal modification using probe molecule-synchrotron X-ray powder diffraction, Appl. Catal., A 596 (2020) 117528.

[10] D. Gao, R.M. Arán-Ais, H.S. Jeon, B. Roldan Cuenya, Rational catalyst and electrolyte design for CO_2 electroreduction towards multicarbon products, Nat. Catal. 2 (2019) 198–210.

[11] L. Mandal, K.R. Yang, M.R. Motapothula, D. Ren, P. Lobaccaro, A. Patra, M. Sherburne, V.S. Batista, B.S. Yeo, J.W. Ager, J. Martin, T. Venkatesan, Investigating the Role of Copper Oxide in Electrochemical CO_2 Reduction in Real Time, ACS Appl. Mater. Interfaces 10 (2018) 8574–8584.

[12] J. Wang, S.H. Kattel, C.J. Hawxhurst, J. Lee, B.M. Tackett, K. Chang, I. Rui, C.-J. Liu, J.G. Chen, Enhancing Activity and Reducing Cost for Electrochemical Reduction of CO_2 by Supporting Palladium on Metal Carbides, Angew. Chem. Int. Ed. 58 (2019) 6271–6275.

[13] S. Zhang, Y. Zhao, Y. Miao, Y. Xu, J. Ran, Z. Wang, Y. Weng, T. Zhang, Understanding Aerobic Nitrogen Photooxidation on Titania through In Situ Time-Resolved Spectroscopy, Angew. Chem. Int. Ed. (2022) Accepted manuscript. https://doi.org/10.1002/anie.202211469

[14] J. Gao, H. Zhang, X. Guo, J. Luo, S.M. Zakeeruddin, D. Ren, M. Grätzel, Selective C-C Coupling in Carbon Dioxide Electroreduction via Efficient Spillover of Intermediates As Supported by Operando Raman Spectroscopy, J. Am. Chem. Soc. 141 (2019) 18704–18714.

[15] L. Ma, N. Liu, B. Mei, K. Yang, B. Liu, K. Deng, Y. Zhang, H. Feng, D. Liu, J. Duan, Z. Jiang, H. Yang, Q. Li, In Situ-Activated Indium Nanoelectrocatalysts for Highly Active and Selective CO_2 Electroreduction around the Thermodynamic Potential, ACS Catal. 12 (2022) 8601–8609.

[16] T.L. Chen, H.C. Chen, Y.P. Huang, S.C. Lin, C.H. Hou, H.Y. Tan, C.W. Tung, T.S. Chan, J.J. Shyue, H.M. Chen, In situ unraveling of the effect of the dynamic chemical state on selective CO_2 reduction upon zinc electrocatalysts, Nanoscale 12 (2020) 18013–18021.

[17] J.Y. Ye, Y.X. Jiang, T. Sheng, S.G. Sun, In-situ FTIR spectroscopic studies of electrocatalytic reactions and processes, Nano Energy 29 (2016) 414–427.

[18] H. Li, P. Wei, D. Gao, G. Wang, In situ Raman spectroscopy studies for electrochemical CO_2 reduction over Cu catalysts, Curr. Opin. Green Sustainable Chem. 34 (2022) 100589.

[19] Y. Zhu, J. Wang, H. Chu, Y.C. Chu, H.M. Chen, In Situ/ Operando Studies for Designing Next-Generation Electrocatalysts, ACS Energy Lett. 5 (2020) 1281–1291.

[20] H. Khan, A.S. Yerramilli, A. D'Oliveira, T.L. Alford, D.C. Boffito, G.S. Patience, Experimental methods in chemical engineering: X-ray diffraction spectroscopy—XRD, Can J Chem Eng. 98 (2020) 1255–1266.

[21] C.F. Holder, R.E. Schaak, Tutorial on Powder X-ray Diffraction for Characterising Nanoscale Materials, ACS Nano 13 (2019) 7359–7365.

[22] J. Lipp, R. Banerjee, M.F. Patwary, N. Patra, A. Dong, F. Girgsdies, S.R. Bare, J.R. Regalbuto, Extension of Rietveld Refinement for Benchtop Powder XRD Analysis of Ultrasmall Supported Nanoparticles, Chem. Mater. 34, (2022) 8091–8111.

[23] A.A. Bunaciu, E. gabriela Udriştioiu, H.Y. Aboul-Enein, X-Ray Diffraction: Instrumentation and Applications, Minerals 45 (2015) 289–299.

[24] A. Ali, Y.W. Chiang, R.M. Santos, X-ray Diffraction Techniques for Mineral Characterization: A Review for Engineers of the Fundamentals, Applications, and Research Directions, Minerals 12 (2022) 205.

*[25] Y. Zheng, A. Vasileff, X. Zhou, Y. Jiao, M. Jaroniec, S.-Z. Qiao, Understanding the Roadmap for Electrochemical Reduction of CO_2 to Multi-Carbon Oxygenates and Hydrocarbons on Copper-Based Catalysts, J. Am. Chem. Soc. 141 (2019) 7646–7659.

By providing some typical examples illustrating the benefit of combining theoretical calculations, surface characterisation, and electrochemical measurements, the authors addressed some issues of the ongoing debates towards better understanding electrochemical reduction of CO_2 at the atomic level.

**[26] Q. Lei, L. Huang, J. Yin, B. Davaasuren, Y. Yuan, X. Dong, Z.P. Wu, X. Wang, K.X. Yao, X. Lu, Y. Han, Structural evolution and strain generation of derived-Cu catalysts during CO_2 electroreduction, Nat. Commun. 13 (2022) 4857.

The authors employed combined, primarily, operando PXRD and Raman spectroscopy to establish correlations between Cu precursors, lattice strains, and catalytic behaviours, demonstrating the unique ability of operando characterisation in studying electrochemical processes.

[27] L. Feng, R. Wang, Y. Zhang, S. Ji, Y. Chuan, W. Zhang, B. Liu, C. Yuan, C. Du, In situ XRD observation of CuO anode phase conversion in lithium-ion batteries, J. Mater. Sci. 54 (2019) 1520–1528.

[28] G.V. Krishnamurthy, M. Chirumamilla, S.S. Rout, K.P. Furlan, T. Krekeler, M. Ritter, H.W. Becker, A.Y. Petrov, M. Eich, M. Störmer, Structural degradation of tungsten sandwiched in hafnia layers determined by in-situ XRD up to 1520 °C, Scientific Reports 11 (2021) 3330.

[29] A. Telfah, Q.M. al Bataineh, M.S. Mousa, A. Ababneh, D. Sadiq, C.J. Tavares, R. Hergenröder, HR MAS NMR, dielectric impedance and XRD characterisation of polyethylene oxide films for structural phase transitions, Physica. B. Condens. Matter 646 (2022) 414353.

[30] W. Sheng, S. Kattel, S. Yao, B. Yan, Z. Liang, C.J. Hawxhurst, Q. Wu, J.G. Chen, Electrochemical reduction of CO_2 to synthesis gas with controlled CO/H_2 ratios, Energy Environ. Sci. 10 (2017) 1180–1185.

[31] J.S. Hardy, J.W. Templeton, D.J. Edwards, Z. Lu, J.W. Stevenson, Lattice expansion of LSCF-6428 cathodes measured by in situ XRD during SOFC operation, J. Power Sources 198 (2012) 76–82.

[32] C. Li, S. Yan, J. Fang, C. Li, S. Yan, + J Fang, Construction of Lattice Strain in Bimetallic Nanostructures and Its Effectiveness in Electrochemical Applications, Small 17 (2021) 2102244.

[33] L.M. Darabian, G.R. Gonçalves, M.A. Schettino, E.C. Passamani, J.C.C. Freitas, Synthesis of nanostructured iron oxides and study of the thermal crystallisation process using DSC and in situ XRD experiments, Mater. Chem. Phys. 285 (2022) 126065.

[34] Q. Ma, C. Hu, K. Liu, S.F. Hung, D. Ou, H.M. Chen, G. Fu, N. Zheng, Identifying the electrocatalytic sites of nickel disulfide in alkaline hydrogen evolution reaction, Nano Energy 41 (2017) 148–153.

**[35] L. Zhai, T.W. Benedict Lo, Z.-L. Xu, J. Potter, J. Mo, X. Guo, C.C. Tang, S.C. Edman Tsang, S.P. Lau, In Situ Phase Transformation on Nickel-Based Selenides for Enhanced Hydrogen Evolution Reaction in Alkaline Medium, ACS Energy Lett. 5 (2020) 2483–2491.

The authors primarily employed operando synchrotron PXRD with a specifically designed transmission cell to investigate the real active species in NiSe2-based catalysts.

[36] Y. Zhang, L. Gao, E.J.M. Hensen, J.P. Hofmann, Evaluating the Stability of Co_2P Electrocatalysts in the Hydrogen Evolution Reaction for Both Acidic and Alkaline Electrolytes, ACS Energy Lett. 3 (2018) 1360–1365.

[37] J. Guo, W. Zhang, L.H. Zhang, D. Chen, J. Zhan, X. Wang, N.R. Shiju, F. Yu, Control over Electrochemical CO_2 Reduction Selectivity by Coordination Engineering of Tin Single-Atom Catalysts, Adv. Sci. 8 (2021) 2102884.

[38] C. Chen, X. Yan, Y. Wu, S. Liu, X. Sun, Q. Zhu, R. Feng, T. Wu, Q. Qian, H. Liu, L. Zheng, J. Zhang, B. Han, The in situ study of surface species and structures of oxide-derived copper catalysts for electrochemical CO_2 reduction, Chem. Sci. 12 (2021) 5938–5943.

[39] A. Dutta, I.Z. Montiel, K. Kiran, A. Rieder, V. Grozovski, L. Gut, P. Broekmann, A tandem (Bi_2O_3 → BiMet) catalyst for highly efficient EC-CO_2 conversion into formate: Operando Raman spectroscopic evidence for a reaction pathway change, ACS Catal. 11 (2021) 4988–5003.

[40] H. Zhang, C. Xu, X. Zhan, Y. Yu, K. Zhang, Q. Luo, S. Gao, J. Yang, Y. Xie, Mechanistic insights into CO_2 conversion chemistry of copper bis-(terpyridine) molecular electrocatalyst using accessible operando spectrochemistry, Nat. Commun. 13 (2022) 6029.

[41] J. Wang, H.U.-Y. Tan, Y. Zhu, H. Chu, H.M. Chen, Linking the Dynamic Chemical State of Catalysts with the Product Profile of Electrocatalytic CO_2 Reduction, Angew. Chem. Int. Ed. 133 (2021) 17394–17407.

[42] S. Nie, S.R. Emory, Probing Single Molecules and Single Nanoparticles by Surface-Enhanced Raman Scattering, Science. 275 (1997) 1102–1106.

[43] E.J. Blackie, E.C. le Ru, P.G. Etchegoin, Single-molecule Surface-enhanced Raman Spectroscopy of Nonresonant Molecules, J. Am. Chem. Soc. 131 (2009) 14466–14472.

**[44] A.D. Handoko, F. Wei, Jenndy, B.S. Yeo, Z.W. Seh, Understanding heterogeneous electrocatalytic carbon dioxide reduction through operando techniques, Nat. Catal. 1 (2018) 922–934.

The authors provided some recent mechanistic understanding using operando optical, X-ray and electron-based techniques.

[45] Y. Zhou, Y. Yao, R. Zhao, X. Wang, Z. Fu, D. Wang, H. Wang, L. Zhao, W. Ni, Z. Yang, Y.-M. Yan, Stabilisation of Cu^+ via Strong Electronic Interaction for Selective and Stable CO_2 Electroreduction, Angew. Chem. Int. Ed. 134 (2022) e202205832.

[46] B. Deng, M. Huang, K. Li, X. Zhao, Q. Geng, S. Chen, H. Xie, X. Dong, H. Wang, F. Dong, The Crystal Plane is not the Key Factor for CO_2-to-Methane Electrosynthesis on Reconstructed Cu_2O Microparticles, Angew. Chem. Int. Ed. 61 (2022) e202114080.

[47] H. Li, P. Wei, D. Gao, G. Wang, In situ Raman spectroscopy studies for electrochemical CO_2 reduction over Cu catalysts, Curr. Opin. Green Sustainable Chem. 34 (2022) 100589.

**[48] M. He, X. Chang, T.-H. Chao, C. Li, I. William A. Goddard, M.-J. Cheng, B. Xu, Q. Lu, Selective Enhancement of Methane Formation in Electrochemical CO_2 Reduction Enabled by a Raman-Inactive Oxygen-Containing Species on Cu, ACS Catal. 27 (2022) 6036–6046.

The authors demonstrated that an oxygen-containing species on Cu-based catalysts can enhance the rate of the CO2RR but also tune selectivities for certain products.

**[49] H. An, L. Wu, L.D.B. Mandemaker, S. Yang, J. de Ruiter, J.H.J. Wijten, J.C.L. Janssens, T. Hartman, W. van der Stam, B.M. Weckhuysen, Sub-Second Time-Resolved Surface-Enhanced Raman Spectroscopy Reveals Dynamic CO Intermediates during Electrochemical CO_2 Reduction on Copper, Angew. Chem. Int. Ed. 60 (2021) 16576–16584.

By using sub-second time-resolved surface-enhanced Raman spectroscopy, the authors correlated a dynamic CO intermediate below 2060 cm^{-1} with CO-CO coupling and ethylene formation, and a static CO intermediate with a vibration mode at 2092 cm^{-1} relates to CO production.